

## Novel Complexes with a Short Tungsten–Phosphorus Triple Bond

Peter Kramkowski,<sup>[a]</sup> Gerhard Baum,<sup>[a]</sup> Udo Radius,<sup>[a]</sup>  
Martin Kaupp,<sup>[b]</sup> and Manfred Scheer\*<sup>[a]</sup>

Dedicated to Professor Helmut Werner on the occasion of his 65th birthday

**Abstract:** [thf(ArO)<sub>3</sub>W≡P → M(CO)<sub>5</sub>] (**3a,b**) (M = W, Cr; Ar = 2,6-Me<sub>2</sub>C<sub>6</sub>H<sub>3</sub>) are prepared by treatment of [W<sub>2</sub>(OAr)<sub>6</sub>] with *t*BuC≡P in the presence of [M(CO)<sub>5</sub>thf]. With 2.127(2) Å **3a** reveals the shortest W≡P triple bond length reported so far. Theoretical calculations employing BP86 density functional methods on the model compounds [(HO)<sub>3</sub>W≡P] (**3c**), [(HO)<sub>3</sub>W≡P → W(CO)<sub>5</sub>] (**3d**), and [thf(HO)<sub>3</sub>W≡P → W(CO)<sub>5</sub>] (**3e**) show a shortening of the W≡P bond due to coordination of the phosphido phosphorus lone pair in **3c** to a [W(CO)<sub>5</sub>] fragment; this is accompanied by a rehybridization of the lone pair on the P atom from sp<sup>0.14</sup> to sp<sup>0.98</sup> in **3d**.

The coordination of the Lewis base THF through the low-lying LUMO+1 σ\*-type orbital leads to an elongation of this triple bond. The phosphido complexes **3a** and **3b** reveal a high side-on reactivity. Thus, the reductive dimerization of **3a** at ambient temperature in toluene yields [W<sub>2</sub>(OAr)<sub>4</sub>{(μ,η<sup>2</sup>:η<sup>1</sup>-P)-W(CO)<sub>5</sub>}<sub>2</sub>] (**7**), which contains a planar [W<sub>4</sub>P<sub>2</sub>] core. The reaction of **3a** with [(ArO)<sub>4</sub>W=O] leads to the novel complex [thf(ArO)<sub>5</sub>W<sub>2</sub>{(μ,η<sup>2</sup>:η<sup>1</sup>-P)W(CO)<sub>5</sub>-(μ-O)] (**8**) with an almost planar

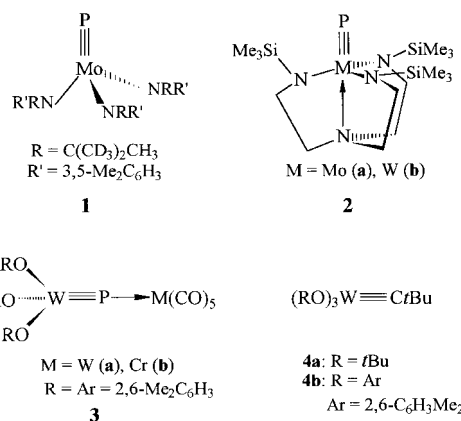
[W<sub>2</sub>OP] four-membered ring system. Furthermore, the phosphido complex **3a** reacts with [(PPh<sub>3</sub>)<sub>2</sub>Pt(η<sup>2</sup>-C<sub>2</sub>H<sub>4</sub>)] to give the dinuclear complex [(ArO)<sub>2</sub>WPt-(PPh<sub>3</sub>)(μ-PPh<sub>2</sub>){(μ-PPh)W(CO)<sub>5</sub>}] (**10**), which also possesses a planar WP<sub>2</sub>Pt four-membered-ring unit. During this reaction an unusual 1,3-Ph shift occurs to give this phosphinidene derivative. Density functional calculations on the simplified model compound [(HO)<sub>3</sub>W(μ-PH<sub>2</sub>)(μ-PH{W(CO)<sub>5</sub>})Pt-(PH<sub>3</sub>)] (**10a**) were applied to gain insight into the bonding situation of the central [WP<sub>2</sub>Pt] core. Population analysis reveals significant W–Pt overlap population for **10a**.

**Keywords:** metathesis • P ligands • phosphido ligands • tungsten

### Introduction

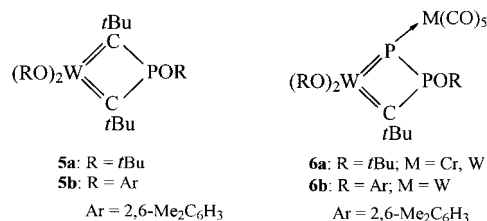
Complexes with a transition metal–phosphorus triple bond are a new class of compounds.<sup>[1]</sup> The first structurally characterized examples **1** and **2** were synthesized in the groups of Cummins<sup>[2]</sup> and Schrock,<sup>[3]</sup> respectively. In these compounds the metal–phosphorus triple bond is kinetically stabilized by bulky amido ligands. Therefore, these compounds reveal exclusively end-on reactivity.<sup>[4]</sup>

Our work, however, has been focused on the synthesis and isolation of the RO-substituted complexes **3** (R = *t*Bu), containing the 15 VE (valence electron) fragment {(RO)<sub>3</sub>W} bound to a phosphido phosphorus atom.<sup>[5]</sup> The synthetic route



[a] Prof. Dr. M. Scheer, Dr. P. Kramkowski, G. Baum, Dr. U. Radius  
Institut für Anorganische Chemie der Universität Karlsruhe  
D-76128 Karlsruhe (Germany)  
Fax: (+49) 721-661921  
E-mail: mascheer@achim6.chemie.uni-karlsruhe.de

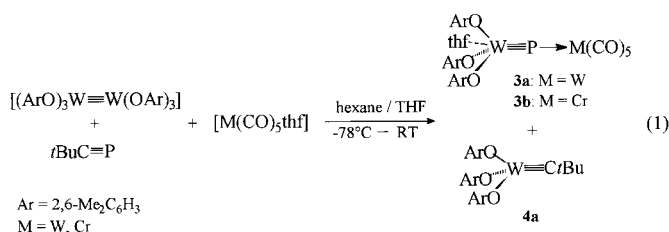
[b] Priv.-Doz. Dr. M. Kaupp  
Max-Planck-Institut für Festkörperforschung Stuttgart  
D-70569 Stuttgart (Germany)  
Fax: (49) 711-689-17-02  
E-mail: kaupp@vsibm1.mpi-stuttgart.mpg.de



employed is the metathesis reaction of  $[\text{W}_2(\text{O}t\text{Bu})_6]$  with  $t\text{BuC}\equiv\text{P}^{[6]}$  in the presence of  $[\text{M}(\text{CO})_5\text{thf}]$  ( $\text{M} = \text{W}, \text{Cr}$ ). The resulting compounds of the type  $[(t\text{BuO})_3\text{W}\equiv\text{P}]$  are stabilized by the coordination of the phosphorus lone pair to a Lewis acidic carbonyl complex fragment  $\{\text{M}(\text{CO})_5\}$ . In contrast to complexes of type **1** and **2**, a high side-on reactivity can be achieved owing to the flexibility of the alkoxide ligands in the complexes **3**. This feature, however, was a disadvantage in the synthesis of these compounds by the metathesis reaction. The reaction led to inseparable mixtures, which contained the desired phosphido compounds **3** ( $\text{R} = t\text{Bu}$ ) and the corresponding alkyldiyne complex **4a** as well as the four-membered ring derivatives **5a** and **6a**.<sup>[7]</sup> The last two arise from a subsequent cycloaddition of the target compounds **3** ( $\text{R} = t\text{Bu}$ ) with an additional equivalent of phosphalkyne followed by a 1,3-*O*tBu shift. Therefore, we were interested in a synthetic procedure that yields complexes of type **3** free of side products. After intensive synthetic efforts we developed an efficient route to the phosphido compounds  $[\text{thf}(\text{ArO})_3\text{W}\equiv\text{P} \rightarrow \text{M}(\text{CO})_5]$  (**3**) ( $\text{M} = \text{W}$  (**a**),  $\text{Cr}$  (**b**),  $\text{Ar} = 2,6\text{-Me}_2\text{C}_6\text{H}_3$ ) starting from  $[\text{W}_2(\text{OAr})_6]$ . Structural and spectroscopic features of the phosphido complexes **3**, as well as initial investigations revealing aspects of the broad reaction potential of these compounds, are reported herein. Density functional calculations have been carried out on model systems of **3** in order to understand better the donor properties of the  $[(\text{ArO})_3\text{W}\equiv\text{P}]$  „ligand“ as well as the side-on reactivity of the complexes. Further calculations examine the electronic structure of a dinuclear reaction product.

## Results and Discussion

The decisive step to overcome the problem of the consecutive reactions of the target molecule **3** was the increase of the steric demand at the alkoxide by employing  $[\text{W}_2(\text{OAr})_6]$  ( $\text{Ar} = 2,6\text{-Me}_2\text{C}_6\text{H}_3$ ). Furthermore, the correct reaction procedure is of crucial importance. For a maximum yield of the phosphido complexes **3** the reaction between  $[\text{W}_2(\text{OAr})_6]$  and  $t\text{BuC}\equiv\text{P}$  in the presence of  $[\text{M}(\text{CO})_5\text{thf}]$  ( $\text{M} = \text{W}, \text{Cr}$ ) must be performed at low temperature until all phosphalkyne has been used in the metathesis reaction. Then the mixture is allowed to warm up to ambient temperature, and the only detectable side product is small quantities of **6b**; the formation of **5b** is no longer observed. The total amount of side-products formed is thus reduced to 5–10 % [Eq. (1)].



After work-up, the phosphido complexes **3a** and **3b** can be obtained as red crystalline compounds in 66 and 53 % isolated yield, respectively. The Lewis basicity of the ArO ligands appears to be insufficient to compensate for the electron

deficiency at the tungsten atom, and coordination of an additional THF molecule becomes necessary. All attempts to isolate THF-free products have failed so far. The complexes **3a** and **3b** are readily soluble in *n*-hexane, toluene, and THF and are extremely sensitive to oxygen and moisture.

**Spectroscopic properties of the phosphido complexes:** The  $^{31}\text{P}\{^1\text{H}\}$  NMR spectrum of **3a** exhibits a singlet at  $\delta = 718.5$  with two pairs of tungsten satellites. The coupling constants are 562.5 Hz for the  $\text{W}\equiv\text{P}$  triple bond and 170.2 Hz for the coordinative bond of phosphorus to the  $\text{W}(\text{CO})_5$  moiety (**3b**:  $\delta = 773.4$ ,  $^1J_{\text{WP}} = 549.3$  Hz; Figure 1). The magnitude of the

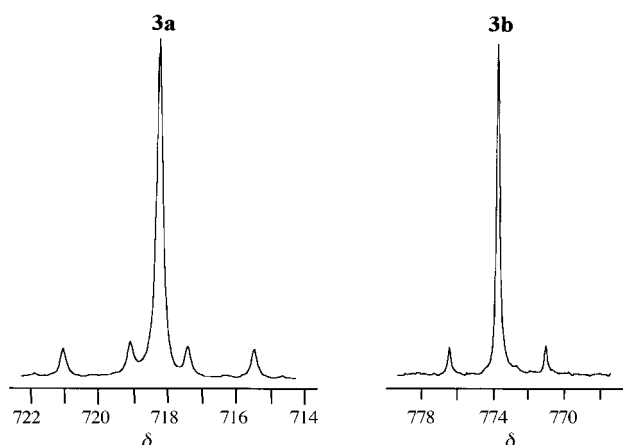


Figure 1.  $^{31}\text{P}\{^1\text{H}\}$  NMR resonances of the phosphido complexes **3a** and **3b** in  $[\text{D}_6]\text{benzene}$  ( $\text{SF} = 101.3$  MHz,  $T = 300$  K)

$^1J_{\text{WP}}$  of the triple bond is in accordance with data found for the  $\text{GaCl}_3$  ( $^1J_{\text{WP}} = 712$  Hz)<sup>[4d]</sup> and  $\text{W}(\text{CO})_5$  ( $^1J_{\text{WP}} = 450, 135$  Hz)<sup>[8]</sup> adducts of the phosphido complex **2b**. These large coupling constants are due to an increase in the s character of the  $\text{W}\equiv\text{P}$  triple bond caused by the linear coordination of the lone pair of the phosphido phosphorus to Lewis acids.<sup>[8, 9]</sup> In the IR spectra of **3a** and **3b**, the appropriate  $A_1'$  band of the CO-stretching frequencies [local  $C_{4v}$  symmetry at the  $\text{LM}(\text{CO})_5$  complex] reveals that the  $\pi$ -acceptor ability of the  $[\text{thf}(\text{RO})_3\text{W}\equiv\text{P}]$  moiety is between that of  $\text{PX}_3$  ( $\text{X} = \text{halogen}$ ) and  $\text{P}(\text{OR})_3$ .<sup>[10]</sup>

**Crystal structure of 3a:** The X-ray structure of **3a** (Figure 2) shows a molecule with an almost linear  $\text{W}(1)\text{-P-W}(2)$  axis of  $176.30(6)^\circ$  in which the ArO ligands protect the  $\text{W}\equiv\text{P}$  triple bond by surrounding it. This orientation towards the  $\text{W}\equiv\text{P}$  triple bond [average angle  $\text{W}(2)\text{-O-C} = 132.6(3)^\circ$ ] is a common feature in alkyldiyne complexes of the type  $[(\text{RO})_3\text{W}\equiv\text{CR}']$  ( $\text{R} = t\text{Bu}$ ,  $\text{R}' = \text{Ph}$ ).<sup>[11]</sup> In **3a** the triple bond length between W2 and P is 2.127(2) Å and, therefore, the shortest  $\text{W}\equiv\text{P}$  bond reported so far.<sup>[12]</sup> The coordinative bond  $\text{W}(1)\text{-P}$  of 2.432(1) Å is relatively short as well.<sup>[13]</sup>

**Quantum chemical calculations on model systems of the phosphido complexes 3:** Density functional calculations on the simplified model systems  $[(\text{HO})_3\text{W}\equiv\text{P}]$  (**3c**),  $[(\text{HO})_3\text{W}\equiv\text{P} \rightarrow \text{W}(\text{CO})_5]$  (**3d**) and  $[\text{thf}(\text{HO})_3\text{W}\equiv\text{P} \rightarrow \text{W}(\text{CO})_5]$  (**3e**), were performed employing the BP86 functional<sup>[14]</sup> and

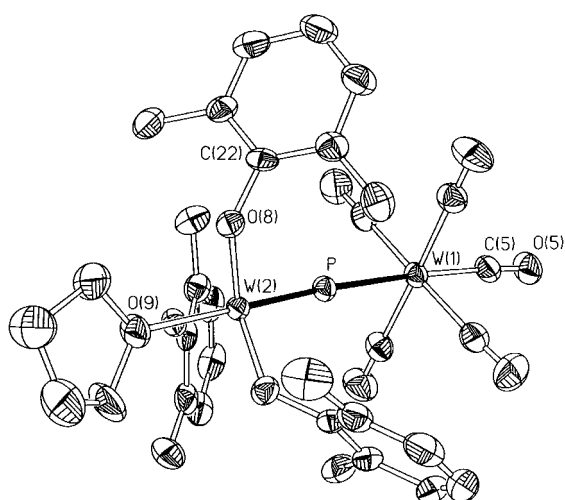


Figure 2. Molecular structure of **3a** (ellipsoids drawn at of 50 % probability level). Selected bond lengths [Å] and angles [°]: W(1)–P 2.4315(13), W(2)–P 2.1261(12), W(2)–O(6) 1.898(3), W(2)–O(9) 2.333(3), O(6)–C(6) 1.382(6), W(1)–P–W(2) 176.30(6), P–W(2)–O(9) 179.50(10), P–W(1)–C(5) 177.0(2), O(6)–W(2)–P 101.52(10), C(6)–O(6)–W(2) 135.0(3), C(14)–O(7)–W(2) 128.9(3), C(22)–O(8)–W(2) 133.8(3).

the Gaussian 94 program.<sup>[15]</sup> We used a quasi-relativistic pseudopotential and a corresponding 6s5p3d valence basis set for W,<sup>[16]</sup> effective-core potentials and DZP valence basis sets for P, O, and C,<sup>[17]</sup> and a DZ basis for H.<sup>[18]</sup> While the structures of **3c** and **3d** were fully optimized, the angles of the hydroxy H atoms in **3e** were held at a W–O–H angle of 126° to avoid H bridges between the THF ligand and the hydroxy groups. Natural population and natural localized molecular orbital analyses<sup>[19]</sup> were carried out using the built-in NBO routines of the Gaussian 94 code.<sup>[15]</sup>

The optimized W≡P distances for the computational models are 2.155 Å for [(HO)<sub>3</sub>W≡P] (**3c**), 2.149 Å for [(HO)<sub>3</sub>W≡P→W(CO)<sub>5</sub>] (**3d**), and 2.167 Å for [thf(HO)<sub>3</sub>W≡P→W(CO)<sub>5</sub>] (**3e**), that is, only slightly longer than the experimentally observed bond length found for **3a** (2.1261(12) Å). The calculated P–W(1) distances in **3d** and **3e** (2.503 Å and 2.499 Å, respectively) are longer than the

experimental ones (2.4315(13) Å). The coordination of the phosphido phosphorus atom to the W(CO)<sub>5</sub> group leads to a slight shortening of the W≡P triple bond, which is accompanied by a considerable rehybridization at the P atom (see below). In contrast, the coordination of THF slightly elongates this bond. The net donor character and *trans* influence of the [(HO)<sub>3</sub>W≡P] „ligand“ are evident from the relative W(1)–C and C–O distances for axial and equatorial carbonyl ligands within the [W(CO)<sub>5</sub>] acceptor, for example, for [thf(HO)<sub>3</sub>W≡P→W(CO)<sub>5</sub>]: W(1)–C<sub>ax</sub> = 2.029 Å, C<sub>ax</sub>–O<sub>ax</sub> = 1.161 Å, W(1)–C<sub>eq</sub> = 2.067 Å, and C<sub>eq</sub>–O<sub>eq</sub> = 1.157 Å (averaged values, see also bonding discussion below).

The analysis of the frontier orbitals (Figures 3 and 4) shows that the highest occupied MOs correspond to an almost degenerate set, predominantly with π(W(2)–P) character, mixed with π(W(1)–C) contributions of the W(CO)<sub>5</sub> unit. The two lowest unoccupied MOs possess mostly π\*(W(2)–P) antibonding character with very large coefficients at the coordinatively unsaturated metal. These π and π\* frontier MOs of **3d** and **3e** derive from the exactly degenerate HOMO and LUMO in free **3c** (of e symmetry in C<sub>3v</sub>). The next lower occupied MO (HOMO – 1) has σ(W(2)–P) character (not shown in Figure 4). The LUMO+1 is a σ\*(W(2)–P) type MO. The high-lying occupied MOs illustrate the donor function of the W≡P bond towards the W(CO)<sub>5</sub> acceptor. In contrast, the three low-lying unoccupied MOs are consistent with the coordinatively unsaturated character of the [(HO)<sub>3</sub>W≡P] part of the complex, and they are well suited to accept electron density from an additional axial donor ligand at this center. This provides a ready explanation for the strong coordination of the THF molecule (calculated bonding energy for THF in **3e**: 54 kJ mol<sup>-1</sup>). Indeed, the coordination of THF in **3e** increases the energy of the HOMO–LUMO gap significantly relative to **3d** (Figure 3). The domination of the components of the W≡P triple bond in both occupied and unoccupied frontier orbitals of **3e** is also consistent with the high side-on reactivity of **3a**.

Atomic and fragment charges obtained from natural population analyses for the model systems are provided in Table 1. They show clearly that in both **3d** and **3e** the

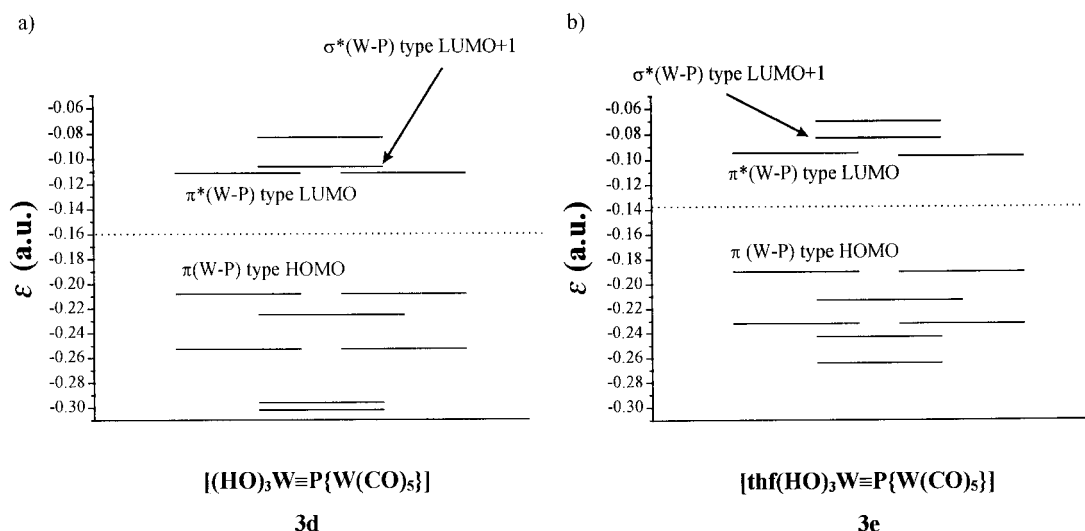


Figure 3. Frontier MO diagrams obtained from the model DFT calculations a) [(HO)<sub>3</sub>W≡P{W(CO)<sub>5</sub>}] (**3d**); b) [thf(HO)<sub>3</sub>W≡P{W(CO)<sub>5</sub>}] (**3e**).

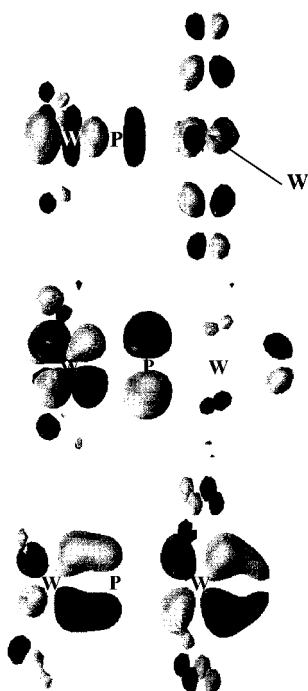


Figure 4. Orbital iso-surfaces (with iso-surface values  $\pm 0.05$  a.u.) for the Frontier Kohn-Sham MOs of  $[(\text{HO})_3\text{WP}(\text{W}(\text{CO})_5)]$ . See Figure 3a for the orbital energies. Bottom: one part of the (almost) degenerate  $\pi(\text{W}2-\text{P})$  type HOMO. Middle: one part of the (almost) degenerate  $\pi^*(\text{W}2-\text{P})$  type LUMO. Top:  $\sigma^*(\text{W}2-\text{P})$  type LUMO+1.

$[(\text{HO})_3\text{W}=\text{P}]$  fragment acts as an efficient electron donor relative to the  $\text{W}(\text{CO})_5$  fragment (the charges indicate more net charge donation than from the carbonyl ligands; the charge is largely withdrawn from the  $\text{W}=\text{P}$  bond). Moreover, the charge donation of the THF donor in **3e** increases the donor ability of this fragment and enhances the negative charge on the  $\text{W}(\text{CO})_5$  unit. The different metal oxidation states of the two fragments are reflected in a positive metal charge for the  $[(\text{HO})_3\text{W}=\text{P}]$  unit and a negative one for the  $\text{W}(\text{CO})_5$  unit. Note that while  $\text{W}(2)$  becomes less positively charged upon THF coordination, the phosphorus atom exhibits a larger positive charge, consistent with an increased polarization of the  $\text{W}(2)=\text{P}$  bond and with increased donation from phosphorus.

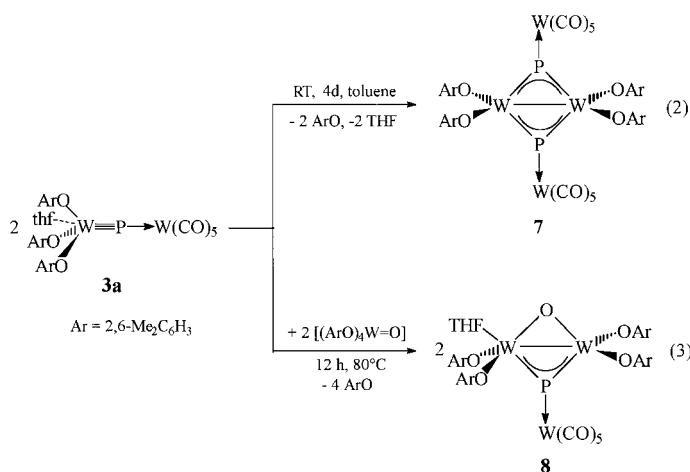
Table 1. Atomic and fragment charges from natural population analyses.

atom/fragment	$[(\text{HO})_3\text{WP}]$ ( <b>3c</b> )	$[(\text{HO})_3\text{WP}(\text{W}(\text{CO})_5)]$ ( <b>3d</b> )	$[\text{thf}(\text{HO})_3\text{WP}(\text{W}(\text{CO})_5)]$ ( <b>3e</b> )
W(2)	+1.101	+1.189	+1.105
P	-0.120	+0.060	+0.131
O (OH) $\text{av}^{[a,b]}$	-0.837	-0.832	-0.841
H (OH) $\text{av}^{[a,b]}$	+0.510	+0.513	+0.502
$[(\text{HO})_3\text{WP}]$	0.000	+0.292	+0.219
(THF) $^{[c]}$			+0.128
W(1)		-1.057	-1.047
C ( $\text{CO}_{\text{ax}}$ ) $^{[d]}$		+0.577	+0.564
O ( $\text{CO}_{\text{ax}}$ ) $^{[d]}$		-0.416	-0.424
C ( $\text{CO}_{\text{eq}}$ ) $\text{av}^{[a,e]}$		+0.565	+0.562
O ( $\text{CO}_{\text{eq}}$ ) $\text{av}^{[a,e]}$		-0.414	-0.421
$[\text{W}(\text{CO})_5]$		-0.292	-0.347

[a] Averaged for groups of atoms. [b] For hydroxy ligands. [c] Summed up for the entire THF ligand. [d] Axial carbonyl ligands. [e] Equatorial carbonyl ligands.

Hybridization analyses of natural localized molecular orbitals (NLMOs) confirm the conclusion of earlier bonding analyses<sup>[8]</sup> about the rehybridization at phosphorus when the  $\text{W}=\text{P}$  bond acts as a donor. Thus, the phosphorus lone-pair NLMO exhibits  $\text{sp}^{0.14}$  hybridization for free  $[(\text{OH})_3\text{W}=\text{P}]$ . This changes to  $\text{sp}^{0.98}$  upon coordination to  $[\text{W}(\text{CO})_5]$ . Correspondingly, the  $\sigma$  contribution to the  $\text{W}=\text{P}$  bond changes from  $\text{sp}^{7.11}$  to  $\text{sp}^{0.51}$  upon coordination. This explains the dramatic changes in the  $^1J_{\text{WP}}$  spin–spin coupling constants.<sup>[8]</sup> A similar rehybridization at phosphorus has been found computationally when the  $\text{M}=\text{P}$  bond donates to a  $\text{BH}_3$  acceptor,<sup>[8]</sup> or when it is transformed into a  $\text{M}=\text{P}-\text{S}$  fragment.<sup>[9]</sup>

**Reactivity studies:** As a result of the high flexibility of the ArO ligands and the relatively weak THF donation, the triple bond in **3** remains accessible and makes these compounds highly side-on reactive. Thus, toluene solutions of **3a** react at ambient temperature over a longer period of time under formal reductive dimerization combined with the loss of two ArO ligands to give dark green crystals of **7** [Eq. (2)]. In the reaction of **3a** with  $[(\text{ArO})_4\text{W}=\text{O}]$ <sup>[20]</sup> the dinuclear compound **8** is formed [Eq. (3)].



Complex **7** appears to be insoluble in *n*-hexane,  $\text{CH}_2\text{Cl}_2$ ,  $\text{Et}_2\text{O}$ , or toluene. In THF or DMSO decomposition is observed at ambient temperature. For the formation of the isolobal carbyne compounds  $[\text{W}_2(\text{Ot-Bu})_4(\mu\text{-CPh})_2]$  by the reaction of  $[\text{W}_2(\text{Ot-Bu})_6]$  with  $\text{PhC}\equiv\text{CR}$ , thermolytic reaction conditions are necessary.<sup>[21]</sup> Complex **8** is the product of a cycloaddition reaction of **3a** with  $[(\text{ArO})_4\text{W}=\text{O}]$  and subsequent reductive W–W bond formation under loss of two ArO ligands.

The molecular structure of **7** (Figure 5) reveals a planar  $\text{W}_4\text{P}_2$  framework with a central  $\text{W}_2\text{P}_2$  ring system. The short W–P bond lengths of 2.269(10) and 2.292(10) Å inside the ring indicate the multiple-bond character of these bonds, whereas the bond lengths of the ring phosphorus to the exocyclic W atom

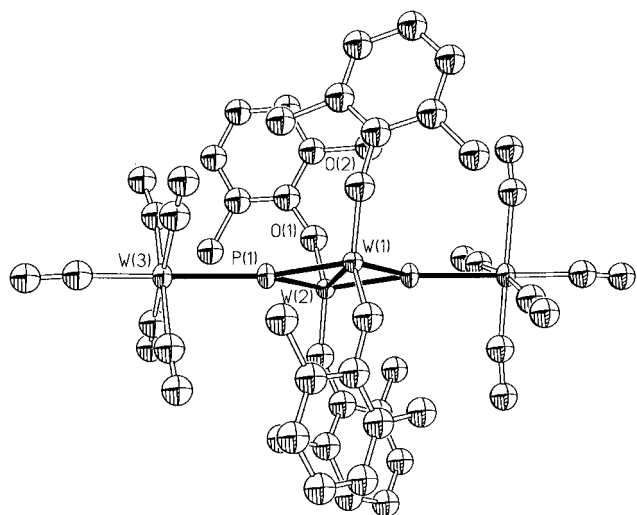


Figure 5. Molecular structure of **7** (ellipsoids drawn at of 50% probability level). Selected bond lengths [Å] and angles [°]: W(1)–W(2) 2.830(1), W(1)–P(1) 2.269(10), W(2)–P(1) 2.292(10), P(1)–W(3) 2.486(2), W(1)–O(2) 1.871(19), O(2)–C(9) 1.381(20), W(2)–O(1) 1.827(29), O(1)–C(1) 1.368(28), W(1)–P(1)–W(2) 76.67(7), P(1)–W(2)–O(1) 108.88(50), P(1)–W(1)–P(1') 104.06(63), O(2)–W(2)–O(2') 109.92(36), O(2)–W(1)–W(2) 123.62(59), W(1)–P(1)–W(3) 132.39(68).

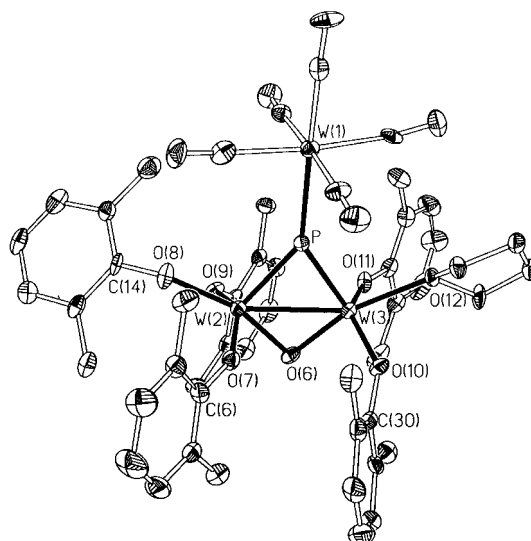
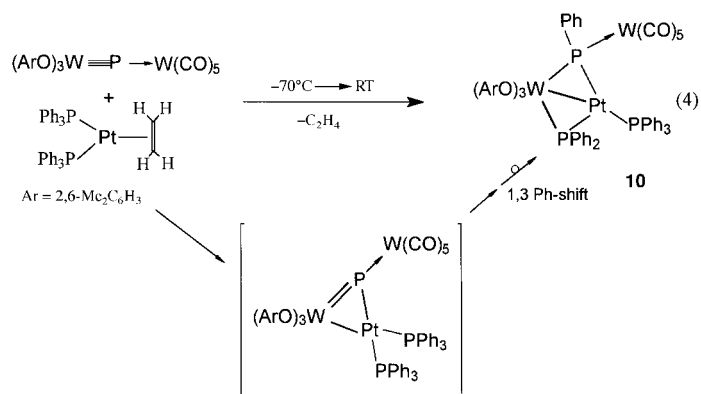


Figure 6. Molecular structure of **8** (ellipsoids drawn at of 30% probability level). Selected bond lengths [Å] and angles [°]: W(2)–W(3) 2.7080(6), W(1)–P 2.519(2), W(2)–P 2.312(2), W(3)–P 2.304(2), W(2)–O(6) 1.960(6), W(3)–O(6) 1.886(7), W(3)–O(12) 2.207(6), W(2)–O(9) 1.928(6), W(3)–O(11) 1.882(6), W(1)–P–W(2) 142.86(10), W(1)–P–W(3) 145.30(10), W(2)–P–W(3) 71.84(7), P–W(3)–W(2) 54.21(6), P–W(3)–O(6) 100.54(18), P–W(2)–W(3) 53.95(5), W(3)–O(6)–W(2) 89.5(2).

(2.486(2) Å) are in range of coordinative bonds of this type.<sup>[13]</sup> The W–W bond is 2.830(1) Å and, therefore, corresponds to a W–W single bond. The six-membered planar framework of **7** is formally comparable to that of the complex [Cp\*Re(CO)<sub>2</sub>(μ,η<sup>2</sup>:η<sup>1</sup>-P)W(CO)<sub>4</sub>]<sub>2</sub> (**9**),<sup>[22]</sup> which also possesses a central [W<sub>2</sub>P<sub>2</sub>] four-membered-ring system. However, in this complex a multiple bond is observed between phosphorus and the exocyclic Re atom, while in **7** the bond to the exocyclic W atom is of coordinative nature. In compound **7**, the endocyclic W–P bond lengths [**9**: *d*(W–P) = 2.439(2) and 2.440(2) Å] as well as the W–W distance [**9**: *d*(W–W) = 3.0523(7) Å] are smaller than in **9**. Pnicogenidene complexes of phosphorus and arsenic similar to **7** were first synthesized and characterized in the group of Huttner.<sup>[23]</sup>

The central motif of the molecular structure of **8** (Figure 6) is the essentially planar W<sub>2</sub>PO ring. The angle between the planes W(2)–W(3)–P and W(2)–W(3)–O(6) is 175.8° and deviates only by 4.2° from planarity. While O(6) and P bind to the tungsten atoms W(2) and W(3) the phosphorus additionally possesses a coordinative bond to a coplanar W(CO)<sub>5</sub> group. The tungsten atoms W(2) and W(3) are symmetrically bridged by the P atom with bond lengths W(2)–P and W(3)–P of 2.312(2) and 2.304(2) Å, respectively; the corresponding bond lengths W(2)–O(6) and W(3)–O(6) differ by 0.074 Å. The bond length W(2)–W(3) is 2.7327(6) Å and, therefore, clearly in the range of W–W single bonds.<sup>[21]</sup>

The phosphido complex **3a** reacts with [(PPh<sub>3</sub>)<sub>2</sub>Pt(C<sub>2</sub>H<sub>4</sub>)] under loss of THF and ethylene to give the novel dinuclear complex **10** in almost quantitative yield as the only phosphorus containing product [Eq. (4)]. The first step of the reaction is presumably a replacement of ethylene by the W–P triple bond, so that an intermediate, such as that indicated in Equation (4), might be formed. Subsequently, an unusual 1,3-shift of one of the phenyl groups of the PPh<sub>3</sub> ligands to the phosphido phosphorus occurs to give bridging PPh<sub>2</sub> and



[PhPW(CO)<sub>5</sub>] groups. However, all attempts to detect the side-on coordinated intermediate by <sup>31</sup>P{<sup>1</sup>H} NMR spectroscopy remained unsuccessful. Therefore, we assume that the rate determining step of the reaction is the formation of the proposed intermediate, which then rearranges quickly through the 1,3-Ph shift within the NMR timescale. Transition metal mediated P–C bond cleavage has been thoroughly investigated, since it is a possible deactivation pathway in homogeneous catalytic processes for catalysts bearing tertiary phosphines in their coordination sphere.<sup>[24]</sup> These processes occur at higher temperatures, while reaction in Equation (4) proceeds at temperatures as low as –10 °C.

The <sup>31</sup>P{<sup>1</sup>H} NMR spectrum of **10** reveals a AMX spinsystem of the P nuclei. The signal at δ = 180.3 (P<sub>A</sub>) is assigned to the phosphorus bearing two phenyl groups, P(2) in Figure 7. Literature data show that signals for μ-PPh<sub>2</sub> moieties bridging metal–metal bonds appear in the downfield region (50 to 300 ppm), whereas upfield resonances (+50 to –200 ppm) occur when these ligands bridge two metal atoms not joined by a bonding interaction.<sup>[25]</sup> The P–P coupling constants are 155 and 29 Hz. The latter arises from the coupling to the PPh<sub>3</sub>

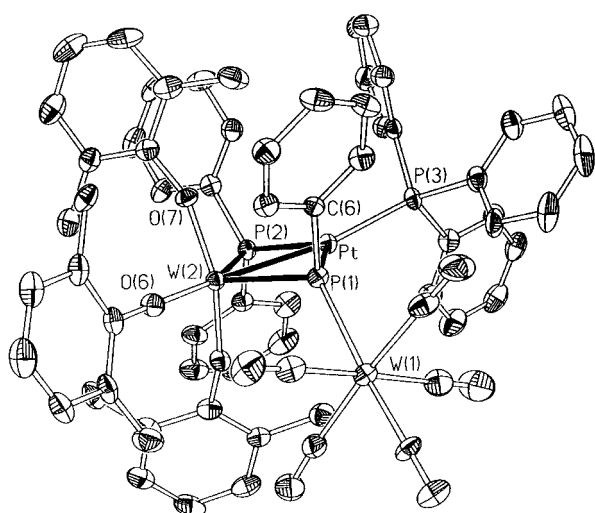


Figure 7. Molecular structure of **10** (ellipsoids drawn at of 30% probability level). Selected bond lengths [Å] and angles [°]: W(2)Pt 2.7360(7), W(2)–P(1) 2.453(2), W(2)–P(2) 2.526(2), Pt–P(1) 2.275(2), Pt–P(2) 2.244(2), Pt–P(3) 2.280(2), W(1)–P(1) 2.604(2), W(2)–O(6) 1.950(6), W(2)–O(7) 1.883(6), W(2)–O(8) 1.856(6), P(1)–C(6) 1.872(9), P(2)–C(42) 1.830(9), P(3)–C(60) 1.832(10), W(2)–P(1)–Pt 70.60(7), W(2)–P(2)–Pt 69.72(6), P(1)–W(2)–P(2) 101.81(7), P(1)–Pt–P(2) 117.54(8), W(1)–P(1)–C(6) 104.7(3), W(2)–O(6)–C(12) 172.2(6), W(2)–O(7)–C(20) 156.6(6), W(2)–O(8)–C(28) 160.2(6).

group at the Pt atom. Owing to the coordination to the  $\{(\text{ArO})_3\text{W}\}$  fragment a  $^1J_{\text{WP}}$  of 178 Hz is observed. The coupling between P(2) and platinum has a value of 2890 Hz. Although the tungsten atom of this ring system is in a high oxidation state, these data for the  $\mu\text{-PPh}_2$  ligand correspond very well to those found in the complex  $[(\text{CO})_4\text{W}(\mu\text{-PPh}_2)_2\text{Pt}(\text{PPh}_3)]$  (**11**) ( $\delta = 173.8$ ,  $^1J_{\text{PtP}} = 2659$  Hz), which is similar to **10**.<sup>[26]</sup> The signal at  $\delta = 166.2$  ( $\text{P}_\text{M}$ ) can be assigned to the phosphinidene P atom bearing one phenyl group and a  $\text{W}(\text{CO})_5$  entity, P(1) in Figure 7. Two P–P couplings are observed for this signal, with coupling constants of 155 and 12 Hz for the coupling of phosphorus to the bridging  $\text{PPh}_2$  group and the end-on bound  $\text{PPh}_3$  at platinum, respectively. The coupling between P(1) and platinum is 1654 Hz, and between P(1) and the coordinated  $\text{W}(\text{CO})_5$  group is 182 Hz. This is consistent for a  $^1J_{\text{WP}}$  coupling of an end-on coordinated phosphorus.<sup>[27]</sup> The signal observed at  $\delta = 75.5$  ( $\text{P}_\text{X}$ ) reveals the appropriate P–P coupling constants of 29 and 12 Hz P(3) in Figure 7. The coupling constant  $^1J_{\text{PtP}}$  is 4310 Hz and lies in between the Pt–P( $\text{Ph}_3$ ) couplings in  $[(\text{PPh}_3)_2\text{Pt}(\text{C}_2\text{H}_4)]$  (3660 Hz)<sup>[28]</sup> and in **11** (5148 Hz).<sup>[26]</sup>

The molecular structure of **10** (Figure 7) confirms the data gained from the  $^{31}\text{P}\{\text{H}\}$  NMR investigation. The central structural element is a planar  $\text{WP}_2\text{Pt}$  moiety. The W(2)–P(1) and W(2)–P(2) bond lengths are 2.453(2) and 2.526(2) Å, respectively; these values correspond to W–P single bonds and coordinative bonds, respectively. The bond lengths Pt–P(1), Pt–P(2), and Pt–P(3) are almost equal (2.275(2), 2.244(2), and 2.279(2) Å, respectively) and consistent with platinum–phosphorus single bonds as observed in  $[(\text{PPh}_3)_2\text{Pt}(\mu\text{-C}_2\text{H}_4)]$ .<sup>[29]</sup> A bond length of 2.604(2) Å between P(1) and W(1) indicates a long coordinative interaction of the phosphorus lone pair with the  $\text{W}(\text{CO})_5$  group.<sup>[13]</sup>

### Quantum chemical calculations on the dinuclear complex **10**:

To gain some insight into the bonding situation of the heteronuclear tungsten–platinum compound **10**, we performed density functional calculations<sup>[30]</sup> on a simplified model of **10**, the complex  $[(\text{HO})_3\text{W}(\mu\text{-PH}_2)(\mu\text{-PH}\{\text{W}(\text{CO})_5\})\text{Pt}(\text{PH}_3)]$  (**10a**). The geometrically optimized compound **10a** is shown in Figure 8, and selected bond lengths and angles are given in the figure caption. The geometry and bonding parameters of the optimized model compound are in good agreement with the experimental structure of **10**.

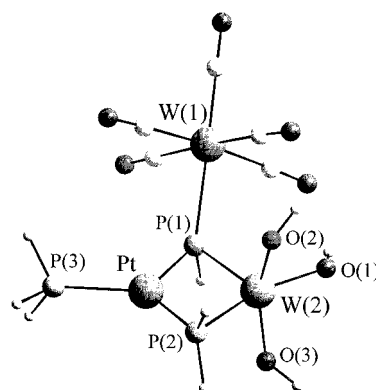


Figure 8. Geometrically optimized structure of  $[(\text{HO})_3\text{W}(\mu\text{-PH}_2)(\mu\text{-PH}\{\text{W}(\text{CO})_5\})\text{Pt}(\text{PH}_3)]$  (**10a**) from RI-J-DFT calculations with B-P86/SVP density functionals. Important calculated bond lengths [Å] and angles [°]: W(2)–Pt 2.797, W(1)–P(1) 2.449, W(1)–P(2) 2.584, W(1)–O(1) 1.966, W(1)–O(2) 1.907, W(1)–O(3) 1.901, W(2)–P(1) 2.604, Pt–P(1) 2.337, Pt–P(2) 2.320, Pt–P(3) 2.306, P(1)–W(1)–P(2) 103.82, P(1)–W(1)–O(1) 99.74, P(1)–W(1)–O(2) 104.24, P(1)–W(1)–O(3) 106.79, O(1)–W(1)–P(2) 156.63, O(2)–W(1)–O(3) 148.70, P(1)–Pt–P(2) 115.72, P(1)–Pt–P(3) 115.63, P(2)–Pt–P(3) 128.59, Pt–P(2)–W(1) 69.31, Pt–P(1)–W(1) 71.48, Pt–P(1)–W(2) 134.30, Pt–W(1)–O(1) 152.13, Pt–W(1)–O(2) 98.37, Pt–W(1)–O(3) 97.21, W(1)–P(1)–Pt–P(2) 5.08.

The calculated W(2)–Pt bond length of 2.797 Å is slightly longer than the experimentally observed one ( $d(\text{W}(2)\text{Pt}) = 2.7360(7)$  Å), but is still in the range of metal–metal bonding distances. In homonuclear phosphanido complexes of the type  $[(\text{CO})_4\text{M}(\mu\text{-PMe}_2)_2\text{M}(\text{CO})_4]$  ( $\text{M} = \text{V}, \text{Cr}, \text{Mn}$ ) synthesized by Vahrenkamp,<sup>[31]</sup> variations in the metal–metal distances from 2.733 Å ( $\text{M} = \text{V}$ ) to 3.675 Å ( $\text{M} = \text{Mn}$ ) have been observed, depending on the electron configuration of the central atom M. In a theoretical study using the extended Hückel method, Hoffmann and co-workers<sup>[32]</sup> assigned a M=M double bond for  $\text{M} = \text{V}$ , a M–M single bond for  $\text{M} = \text{Cr}$ , and no M–M interaction for  $\text{M} = \text{Mn}$  in the different compounds. They put these complexes in a general setting of bridged and unbridged  $\text{M}_2\text{L}_{10}$  compounds. Geoffroy and co-workers<sup>[26]</sup> assigned a W–Pt bond to the complex  $[(\text{OC})_4\text{W}(\mu\text{-PPh}_2)_2\text{Pt}(\text{PPh}_3)]$  (**11**), a compound closely related to **10**. In the following, we want to compare a simplified model for Geoffroy's compound  $[(\text{OC})_4\text{W}(\mu\text{-PH}_2)_2\text{Pt}(\text{PH}_3)]$  (**11a**)<sup>[33]</sup> with our model  $[(\text{HO})_3\text{W}(\mu\text{-PH}_2)(\mu\text{-PH}\{\text{W}(\text{CO})_5\})\text{Pt}(\text{PH}_3)]$  (**10a**).

For the electron count on **11a**, we opt to cleave the metal–ligand bonds of the ring heterolytically and end up with two negatively charged  $[\text{PH}_2]^-$  units, a neutral carbonyl entity  $[(\text{OC})_4\text{W}]$ , and a cationic complex fragment  $[\text{Pt}–\text{PH}_3]^{2+}$ . In **10a** we also find a  $[\text{PH}_2]^-$  and a  $[\text{Pt}–\text{PH}_3]^{2+}$  unit. In contrast to

**11a**, however, the phosphinidene entity  $[\text{PH}\{\text{W}(\text{CO})_5\}]^{2-}$  carries two negative charges, and consequently the tungsten fragment  $[(\text{HO})_3\text{W}]^+$  has a single positive charge with a formal  $d^2$  electron configuration at the central atom. Metal–metal bonding can be envisaged in **10a** and **11a** to arise from donation of an occupied tungsten  $d$  orbital of the  $d^2$  (in **10a**) or  $d^6$  (in **11a**) tungsten atom to an unoccupied acceptor orbital of the  $d^8$  platinum atom. However, the question of direct metal–metal bonding in doubly bridged complexes is controversial, since the bonding interaction between the metal atoms may take place through orbitals involving the bridging atoms (Figure 9).

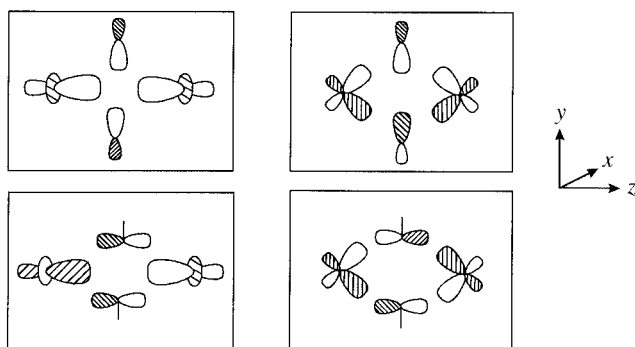


Figure 9. Bonding interactions between metal atoms through orbitals involving the bridging atoms.

Figure 9 depicts some important interactions that build up the  $\sigma$  frame of the four-membered core  $[\text{M}(\mu\text{-PR})_2\text{M}]$ . Whereas phosphorus  $sp_x$  hybrid orbitals are responsible for P–R bonding, the  $[\text{W}(\mu\text{-PR})_2\text{Pt}]$   $\sigma$  frame is mainly a result of the interactions of linear combinations of (occupied)  $sp_y$  and  $p_z$  orbitals with (unoccupied) metal  $[d_{z^2}, s, p_z]$ - and  $[d_{yz}, p_y]$ -hybrid orbitals. For metal–metal bonding, one can think of an interaction of  $[d_{z^2}, s, p_z]$ -hybrid orbitals located on both metal centers, as shown on the upper left of the Figure 9. However, to evaluate metal–metal bonding by means of population analysis, one has to consider multicenter contributions emerging from overlap of the bridging atoms to both metal centers.

A SEN (shared electron number) analysis<sup>[34]</sup> of the covalent contributions to the W–Pt bond in  $[(\text{OC})_4\text{W}(\mu\text{-PH}_2)_2\text{Pt}(\text{PH}_3)]$  (**11a**) gives a shared electron number of 0.251 electrons for W–Pt, which is almost entirely consumed by the multicenter contributions of 0.117 electrons per W–P–Pt bridge. The remaining value of 0.017 electrons indicates that there is no significant tungsten–platinum interaction in this compound. If the same analysis is carried out for  $[(\text{HO})_3\text{W}(\mu\text{-PH}_2)(\mu\text{-PH}\{\text{W}(\text{CO})_5\})\text{Pt}(\text{PH}_3)]$  (**10a**), a shared electron number of 0.489 is calculated for W–Pt; this is significantly higher in comparison with the SEN W–Pt calculated for **11a**. The relevant multicenter contributions in **10a** are on average almost the same as in **11a**, and the net result is a SEN W–Pt of 0.277 electrons. On the basis of the DFT calculations applied here, we can attribute a W–Pt interaction to our model compound **10a**.

## Conclusion

We finally succeeded in the synthesis of the phosphido complexes **3** by using appropriate variations of steric considerations of the tungsten alkoxide dimer and reaction conditions. Thus, these compounds are now available in good preparative yields. The high side-on reactivity is illustrated in the cyclomerization reactions of **3** with itself, with  $[(\text{ArO})_4\text{W}=\text{O}]$ , and with  $[(\text{PPh}_3)_2\text{Pt}(\text{C}_2\text{H}_4)]$  leading to the dinuclear complexes **7**, **8**, and **10**. If both metal-complex fragments possess RO ligands, we observe a strong tendency for those compounds to form metal–metal bonds by reductive ArO elimination. This feature seems to be a common property of these systems.

Current investigations in our laboratories concerning the reactivity of **3a** towards alkynes, nitriles, and related compounds as well as other coordination complexes will definitely offer more insights into the exciting chemistry of this new class of compounds with a metal–phosphorus triple bond.

## Experimental Section

**General techniques:** All reactions were performed under an atmosphere of dry argon using Schlenk and glove box techniques. Solvents were purified and degassed by standard procedures and distilled prior to use. NMR spectra were recorded on a Bruker AC250 [ $^1\text{H}$ : 250.13 MHz;  $^{31}\text{P}$ : 101.256 MHz; standard  $\text{Me}_4\text{Si}$  ( $^1\text{H}$ ), 85 %  $\text{H}_3\text{PO}_4$  ( $^{31}\text{P}$ )]. IR spectra were recorded in Nujol on a Bruker IFS28 FT-IR-spectrometer. MS: Finnigan MAT711 at 70 eV. Correct elemental analysis for the isolated products were performed by the analytical laboratory of the institute.

**Reagents:** Unless otherwise stated, commercial-grade chemicals were used without further purification.  $t\text{BuC}\equiv\text{P}$  was synthesized in accordance to the literature route.<sup>[35]</sup>  $[(\text{ArO})_6\text{W}_2]$  was synthesized as published.<sup>[36]</sup>

**Synthesis of 3a and 3b:** A solution of  $[\text{W}_2(\text{OAr})_6]$  (1.094 g, 1 mmol) and  $[\text{M}(\text{CO})_5\text{thf}]$  (25 mL of a 0.04 M solution prepared by irradiation of  $\text{M}(\text{CO})_6$  in THF;  $\text{M} = \text{W}, \text{Cr}$ ) in THF (25 mL) was cooled to  $-196^\circ\text{C}$ .  $t\text{BuC}\equiv\text{P}$  (2 mL of a 0.5 M solution in *n*-hexane) was cooled to  $-70^\circ\text{C}$  and added to the solid mixture. The solution was allowed to warm to ambient temperature within 15 h. The solvent was removed in vacuo, and the residue was extracted with *n*-hexane (30 mL) and filtered. The solvent of the resulting mixture was then reduced in vacuo until the onset of crystallization. At  $8^\circ\text{C}$  crystals of **3a** suitable for an X-ray single-crystal diffraction study were isolated in the shape of yellow plates which appear red in thicker layers. Isolated yield: 650 mg, 66 % of **3a** and 450 mg, 53 % of **3b**;  $^{31}\text{P}\{^1\text{H}\}$  NMR (101.256 MHz,  $\text{C}_6\text{D}_6$ , 300 K): **3a**:  $\delta = 718.5$  (s,  $^1J_{\text{WP}} = 562.5$  Hz,  $^1J_{\text{WP}} = 170.2$  Hz); **3b**:  $\delta = 773.4$  (s,  $^1J_{\text{WP}} = 549.3$  Hz); IR (Nujol): **3a**:  $\tilde{\nu}(\text{CO}) = 2069$  (s), 1976 (sh), 1947  $\text{cm}^{-1}$  (br); **3b**:  $\tilde{\nu}(\text{CO}) = 2065$  (s), 1985 (sh), 1962  $\text{cm}^{-1}$  (br); EI-MS (70 eV;  $180^\circ\text{C}$ ):  $m/z$  (%): 901.9 (9.6)  $[\text{M} - \text{THF}]^+$ , 818.0 (4.4)  $[\text{M} - 3\text{CO} - \text{THF}]^+$ , 790.0 (2.9)  $[\text{M} - 4\text{CO} - \text{THF}]^+$ , 653.1 (40)  $[(\text{ArO})_3\text{WP} - \text{Me}]^+$ , 351.9 (32.1)  $[\text{W}(\text{CO})_6]^+$ , 72.0 (100)  $[\text{THF}]^+$ .

**Synthesis of 7:** A solution of **3a** (0.5 mmol, 490 mg) in toluene (25 mL) was kept at room temperature. After one day crystals of **7** formed in shape of dark green rhombi (after 4 d, isolated yield: 120 mg, 30 %).  $^{31}\text{P}\{^1\text{H}\}$  NMR ( $[\text{D}_8]\text{THF}$ ,  $-78^\circ\text{C}$ ):  $\delta = 558.2$  (s,  $^1J_{\text{WP}} = 202.7$  Hz); IR (Nujol):  $\tilde{\nu}(\text{CO}) = 2065$  (s), 1939 (br), 1920  $\text{cm}^{-1}$  (sh); EI-MS (70 eV;  $180^\circ\text{C}$ ):  $m/z$  (%): 1561.9 (9)  $[\text{M}]^+$ , 1477.8 (1.1)  $[\text{M} - 3\text{CO}]^+$ , 1238.1 (1.2)  $[\text{M} - \text{W}(\text{CO})_5]^+$ , 1098.1 (4)  $[(\text{ArO})_4\text{W}_3\text{P}_2]^+$ , 351.9 (50.8)  $[\text{W}(\text{CO})_6]^+$ .

**Synthesis of 8:** A solution of **3a** (0.5 mmol, 490 mg) and  $[(\text{ArO})_4\text{W}=\text{O}]$  (0.5 mmol; 342 mg) in toluene (25 mL) was stirred at  $80^\circ\text{C}$  for 12 h. After evaporation of the solvent, the residue was extracted with 20 mL hexane. Besides unreacted  $[(\text{ArO})_4\text{W}=\text{O}]$  it was possible to obtain **8** as black platelets. Owing to the impurities of **8** with starting material a complete spectroscopic characterization of **8** was impossible. However, crystals of **8** could be reproduced from different reactions.

**Synthesis of 10:** The phosphido complex **3a** (0.5 mmol, 490 mg) was dissolved in toluene (25 mL) and cooled to  $-70^{\circ}\text{C}$ . At this temperature  $[(\text{Ph}_3\text{P})\text{Pt}(\eta^2\text{-C}_2\text{H}_4)]$  was added at once. Then the solution was allowed to warm to ambient temperature within 15 h. The solvent was removed in vacuo, and the residue was extracted in *n*-hexane (50 mL). This solution was kept at  $8^{\circ}\text{C}$  to give dark-brown rhombi, which were suitable for an X-ray diffraction study. Upon reduction of the solvent, **10** could be isolated in a total yield of 50 % (400 mg).  $^{31}\text{P}\{^1\text{H}\}$  NMR (101.256 MHz,  $\text{C}_6\text{D}_6$ , 300 K):  $\delta = 180.3$  (dd,  $^2J_{\text{PP}} = 155$ , 29 Hz,  $^1J_{\text{WP}} = 178$  Hz,  $^1J_{\text{PtP}} = 2890$  Hz), 166.2 (dd,  $^2J_{\text{PP}} = 155$ , 12 Hz,  $^1J_{\text{WP}} = 182$  Hz,  $^1J_{\text{PtP}} = 1654$  Hz), 75.5 (dd,  $^2J_{\text{PP}} = 29$ , 12 Hz,  $^1J_{\text{PtP}} = 4310$  Hz); IR (Nujol):  $\tilde{\nu}(\text{CO}) = 2059$  (vs), 1970 (sh), 1945 (vs), 1925 (vs), 1986  $\text{cm}^{-1}$  (vs).

**Crystal structure analysis:** Crystal structure analyses of **3a**, **7**, **8**, and **10** were performed on a STOE STADI IV (**3a**:  $\omega$ -scan mode) and a STOE IPDS (**7**, **8**, **10**, and  $[(\text{ArO})_4\text{W}=\text{O}]$ ) diffractometer with  $\text{MoK}\alpha$  radiation ( $\lambda = 0.71073$  Å), and with empirical absorption corrections for **3a** (6 Psi-scans). The structures were solved by direct methods by use of SHELXS-86.<sup>[37a]</sup> Full-matrix least-squares refinement on  $F^2$  in SHELXL-93<sup>[37b]</sup> was performed with anisotropic displacement for non-H atoms. Hydrogen atoms were located in idealized positions and refined isotropically according to the riding model. Crystallographic data for compounds **3a**, **7**, **8**, and **10** are given in Table 2.

Crystals of **7** suitable for an X-ray diffraction study were directly obtained from the toluene reaction mixture at ambient temperature. Unfortunately, all crystals of the compound appeared to be twinned. Owing to the low solubility in *n*-hexane, toluene, and  $\text{CH}_2\text{Cl}_2$  and the decomposition in THF or DMSO at ambient temperature recrystallization of **7** was impossible. However, the structure could be solved in the orthorhombic space group *Fmmm*. There, the structure could be refined up to a final  $R_1$  value of 0.022 with split positions for the CO and Ar groups. The problem of this solution, however, is that only parts of the structure possess *mmm* symmetry. The W, P, and O atoms of the alkoxy ligand fully obey the *mmm* symmetry, whereas the CO and Ar moieties only adhere to a  $2/m$  symmetry—the CO and Ar groups lie on two different axes. Therefore, four different possibilities arise for the refinement of the structure: i) refinement of the structure in *Fmmm* with disordered CO and Ar groups; ii) resolving the structure under loss of symmetry in *C2/m* with disordered and doubly twinned CO ligands; iii)

assumption of a different position for the Ar moieties and refinement of those as disordered and twinned; iv) the refinement in *P1* under further loss of symmetry with double twinning but without any disorder. In all these solutions one of the methyl groups of the Ar substituent comes very close to one of the CO ligands. Therefore, problems arose for the disordered groups during the anisotropic refinement that could be satisfactorily resolved by the use of appropriate restraints. After thorough consideration of all solutions, we found that the molecular structure of **7** is best described by the refinement in the space group *Fmmm*. In this solution the CO ligands were calculated as being disordered, and the position of the Ar substituents was fixed by restraints. Only the heavy atoms W and P were refined anisotropically.

**Crystallographic data for  $[(\text{ArO})_4\text{W}=\text{O}]$ :**  $\text{C}_{32}\text{H}_{36}\text{O}_5\text{W}$ ,  $M = 684.46$ , crystal size  $0.19 \times 0.08 \times 0.08$  mm<sup>3</sup>, tetragonal, space group *P4/n*;  $a = b = 14.109(2)$  Å,  $c = 7.358(2)$  Å,  $T = 200(2)$  K,  $Z = 2$ ,  $V = 1464.7(4)$  Å<sup>3</sup>,  $\rho_{\text{calcd}} = 1.552$  mg m<sup>-3</sup>,  $\mu(\text{MoK}\alpha) = 39.81$  cm<sup>-1</sup>, 1415 independent reflections ( $2\theta_{\text{max}} = 52^{\circ}$ ), 1314 observed reflections with  $F_o = 4\sigma(F_o)$ ; 90 parameters,  $R_1 = 0.0370$ ,  $wR_2 = 0.0999$ .

Crystallographic data (excluding structure factors) for the structures reported in this paper have been deposited with the Cambridge Crystallographic Data Centre as supplementary publication no. CCDC-116259–116263. Copies of the data can be obtained free of charge on application to CCDC, 12 Union Road, Cambridge CB2 1EZ, UK (fax: (+44) 1223-336-033; e-mail: deposit@ccdc.cam.ac.uk).

## Acknowledgments

The financial support from the Deutsche Forschungsgemeinschaft and the Fonds der Chemischen Industrie is gratefully acknowledged. The authors thank Degussa for the gift of precious metals.

- [1] Reviews: a) M. Scheer, *Angew. Chem.* **1995**, *107*, 2151–2153; *Angew. Chem. Int. Ed. Engl.* **1995**, *34*, 1997–1999; b) *Coord. Chem. Rev.* **1997**, *163*, 271.

Table 2. Crystallographic data for **3a**, **7**, **8**, and **10**.

	<b>3a</b>	<b>7</b>	<b>8 · 2 C<sub>7</sub>H<sub>8</sub></b>	<b>10 · 0.5 C<sub>6</sub>H<sub>14</sub></b>
formula	$\text{C}_{33}\text{H}_{35}\text{O}_9\text{PW}_2$	$\text{C}_{42}\text{H}_{36}\text{O}_{14}\text{P}_2\text{W}_4$	$\text{C}_{63}\text{H}_{66}\text{O}_{12}\text{PW}_3$	$\text{C}_{68}\text{H}_{64}\text{O}_8\text{P}_3\text{PtW}_2$
$M_r$	974.28	1562.05	1597.68	1664.89
crystal size [mm]	$0.42 \times 0.30 \times 0.15$	$0.08 \times 0.08 \times 0.02$	$0.20 \times 0.10 \times 0.02$	$0.15 \times 0.15 \times 0.04$
$T$ [K]	200(2)	200(1)	200(1)	200(1)
space group	<i>P2<sub>1</sub>/n</i> (No. 14)	<i>Fmmm</i> (No. 69)	<i>Pbcn</i> (No. 60)	<i>P2<sub>1</sub>/c</i> (No. 14)
crystal system	monoclinic	orthorhombic	orthorhombic	monoclinic
$a$ [Å]	10.017(2)	18.378(3)	30.413(6)	22.398(4)
$b$ [Å]	18.886(4)	14.731(2)	20.957(4)	14.725(2)
$c$ [Å]	18.407(4)	17.120(3)	19.198(4)	20.120(3)
$\alpha$ [°]	90	90	90	90
$\beta$ [°]	98.17(3)	90	90	108.86(3)
$\gamma$ [°]	90	90	90	90
$V$ [Å <sup>3</sup> ]	3446.9(12)	4634.8(15)	12236(4)	6279(2)
$Z$	4	4	8	4
$\rho_{\text{calcd}}$ [g cm <sup>-3</sup> ]	1.877	2.239	1.735	1.761
$\mu$ [mm <sup>-1</sup> ]	6.766	10.027	5.712	6.008
radiation $\lambda$ [Å]			$\text{MoK}\alpha$ (0.71073)	
diffractometer	STOE STADI IV	STOE IPDS	STOE IPDS	STOE IPDS
$2\theta$ range [°]	$3.1 \leq 2\theta \leq 53.04$	$4.44 \leq 2\theta \leq 51.7$	$3.94 \leq 2\theta \leq 51.66$	$3.64 \leq 2\theta \leq 51.66$
index range	$-12 \leq h \leq 9$ $0 \leq k \leq 23$ $0 \leq l \leq 23$	$-20 \leq h \leq 22$ $-17 \leq k \leq 17$ $-20 \leq l \leq 20$	$-27 \leq h \leq 37$ $-25 \leq k \leq 20$ $-22 \leq l \leq 23$	$-27 \leq h \leq 27$ $-18 \leq k \leq 18$ $-24 \leq l \leq 20$
data/restraints/parameters	6721/0/412	1239/132/135	11323/0/711	12024/0/731
independent reflections with $[I > 2\sigma(I)]$	6234 ( $R_{\text{int}} = 0.0000$ )	1039 ( $R_{\text{int}} = 0.0431$ )	6482 ( $R_{\text{int}} = 0.1299$ )	8702 ( $R_{\text{int}} = 0.1286$ )
goodness-of-fit on $F^2$	1.130	0.972	0.806	0.941
$R_1$ , <sup>[a]</sup> $wR_2$ , <sup>[b]</sup> $[I > 2\sigma(I)]$	0.0289, 0.0705	0.0220, 0.0524	0.0397, 0.0661	0.0525, 0.1149
$R_1$ , <sup>[a]</sup> $wR_2$ , <sup>[b]</sup> (all data)	0.0327, 0.0746	0.0286, 0.0548	0.0917, 0.0754	0.0783, 0.1257
largest diff. peak and hole [ $\text{e} \text{ \AA}^{-3}$ ]	0.783, $-1.268$	1.213, $-0.748$	1.211, $-0.770$	2.877, $-1.856$

[a]  $R_1 = \sum |F_o| - |F_c| / \sum |F_o|$ . [b]  $wR_2 = [\sum w(F_o^2 - F_c^2)^2] / [\sum (F_o^2)^2]^{1/2}$ .



- [2] C. E. Laplaza, W. M. Davis, C. C. Cummins, *Angew. Chem.* **1995**, *107*, 2181; *Angew. Chem. Int. Ed. Engl.* **1995**, *34*, 2042.
- [3] N. C. Zanetti, R. R. Schrock, W. M. Davis, *Angew. Chem.* **1995**, *107*, 2184; *Angew. Chem. Int. Ed. Engl.* **1995**, *34*, 2044.
- [4] a) M. J. A. Johnson-Carr, P. M. Lee, A. L. Odom, W. M. Davis, C. C. Cummins, *Angew. Chem.* **1997**, *109*, 110; *Angew. Chem. Int. Ed. Engl.* **1997**, *36*, 87; b) M. J. A. Johnson, A. L. Odom, C. C. Cummins, *J. Chem. Soc. Chem. Commun.* **1997**, 1523; c) J. A. Johnson-Carr, N. C. Zanetti, R. R. Schrock, *J. Am. Chem. Soc.* **1996**, *118*, 11305; d) M. Scheer, J. Müller, G. Baum, M. Häser, *J. Chem. Soc. Chem. Commun.* **1998**, 1051.
- [5] a) M. Scheer, K. Schuster, T. A. Budzichowski, M. H. Chisholm, W. E. Streib, *J. Chem. Soc. Chem. Commun.* **1995**, 1671; b) M. Scheer, P. Kramkowski, K. Schuster, *Organometallics* **1999**, *18*, 2874
- [6] For the corresponding two-component-reaction without  $[M(CO)_5thf]$  ( $M = Cr, W$ ) see a) G. Becker, W. Becker, R. Knebl, H. Schmidt, U. Hildenbrand, M. Westerhausen, *Phosphorus Sulphur* **1987**, *30*, 349; b) G. Becker, W. Becker, R. Knebl, H. Schmidt, U. Weber, M. Westerhausen, *Nova Acta Leopold.* **1985**, *59*, 55; c) P. Binger, in *Multiple Bonds and Low Coordination in Phosphorus Chemistry* (Ed.: M. Regitz, O. J. Scherer), Thieme, Stuttgart **1990**, p. 100.
- [7] All attempts to separate these mixtures by column chromatography with differently prepared silicagel (activated, deactivated, silanized) and  $Al_2O_3$  failed due to the decomposition of the alkoxide. On biogel® no decomposition, but separation was observed.
- [8] M. Scheer, J. Müller, M. Häser, *Angew. Chem.* **1996**, *108*, 2637; *Angew. Chem. Int. Ed. Engl.* **1996**, *35*, 2492.
- [9] T. Wagener, G. Frenking, *Inorg. Chem.* **1998**, *37*, 1805.
- [10] J. E. Huheey, E. Keiter, R. Keiter, *Inorganic Chemistry, Principles of Structure and Reactivity*, 2nd ed., de Gruyter, Berlin **1995**, pp. 500.
- [11] F. A. Cotton, W. Schmotzer, E. S. Shamsoum, *Organometallics* **1984**, *3*, 1770; K. G. Caulton, R. H. Cayton, M. H. Chisholm, J. C. Huffman, E. B. Lobkovsky, Z. Xue, *Organometallics* **1992**, *11*, 321, and references therein.
- [12] Compare:  $d(WP) = 2.162(4) \text{ \AA}$  in  $[(N_3N)W \equiv P]$  (**2b**),<sup>[3]</sup>  $d(WP) = 2.168(4) \text{ \AA}$  in  $[(N_3N)W \equiv P \rightarrow GaCl_3]$ ,<sup>[4d]</sup>  $d(WP) = 2.202(2) \text{ \AA}$  in  $[trans-W(CO)_4(P \equiv W(N_3N)_2)]$   $[N_3N = N(CH_2CH_2NSiMe_3)_3]$ ,<sup>[8]</sup> and  $d(WP) = 2.169(1) \text{ \AA}$  in  $[(Ph_2MeP)_2Cl_2(CO)W \equiv PAr]$ : A. H. Cowley, B. Pellerin, J. L. Atwood, S. G. Bott, *J. Am. Chem. Soc.* **1990**, *112*, 6734.
- [13] Compare:  $d(WP) = 2.544 \text{ \AA}$  in  $[Ph_3P \rightarrow W(CO)_5]$ : M. J. Aroney, I. E. Buys, M. S. Davies, T. W. Hambley, *J. Chem. Soc. Dalton Trans.* **1994**, 2827;  $\bar{d}(WP) = 2.445(7) \text{ \AA}$  in  $[W(CO)_4(\eta^4-P_4)[W(CO)_5]_4]$ : M. Scheer, E. Hermann, J. Sieler, M. Oehme, *Angew. Chem.* **1991**, *103*, 1023; *Angew. Chem. Int. Ed. Engl.* **1991**, *30*, 969.
- [14] A. D. Becke, *Phys. Rev. A* **1988**, *38*, 3098.
- [15] M. J. Frisch, G. W. Trucks, H. B. Schlegel, P. M. W. Gill, B. G. Johnson, M. A. Robb, J. R. Cheeseman, T. Keith, G. A. Petersson, J. A. Montgomery, K. Raghavachari, M. A. Al-Laham, V. G. Zakrzewski, J. V. Ortiz, J. B. Foresman, C. Y. Peng, P. Y. Ayala, W. Chen, M. W. Wong, J. L. Andres, E. S. Replogle, R. Gomperts, R. L. Martin, D. J. Fox, J. S. Binkley, D. J. Defrees, J. Baker, J. P. Stewart, M. Head-Gordon, C. Gonzalez, J. A. Pople, *Gaussian 94, Revisions B2 and G.2* Gaussian, Pittsburgh, **1995**.
- [16] D. Andrae, U. Häussermann, M. Dolg, H. Stoll, H. Preuss, *Theor. Chim. Acta* **1990**, *77*, 123.
- [17] A. Bergner, M. Dolg, W. Küchle, H. Stoll, H. Preuss, *Mol. Phys.* **1993**, *80*, 1431.
- [18] T. H. Dunning, H. Hay, in *Methods of Electronic Structure Theory; Modern Theoretical Chemistry, Vol. 3* (Ed. H. F. Schaefer III), Plenum, New York, **1977**.
- [19] a) A. E. Reed, F. Weinhold, *J. Chem. Phys.* **1985**, *83*, 1736; b) A. E. Reed, L. A. Curtiss, F. Weinhold, *Chem. Rev.* **1988**, *88*, 899.
- [20] A single crystal X-ray analysis of  $[(ArO)_4W=O]$  established that this compound is the first example for a monomeric square-pyramidal complex of the type  $[X_4W=O]$  [ $d(W=O) = 1.704(7) \text{ \AA}$ ] without any intermolecular  $O \rightarrow W$  contacts ( $5.655 \text{ \AA}$ ); compare:  $[X_4W=O]$  ( $X = Cl, Br$ ): U. Müller, *Acta Crystallogr. C* **1984**, *40*, 915, and references therein.
- [21] F. A. Cotton, W. Schwozter, E. S. Shamsoum, *Organometallics* **1983**, *2*, 1167; F. A. Cotton, W. Schwozter, E. S. Shamsoum, *J. Organomet. Chem.* **1985**, *296*, 55;  $[W_2(OtBu)_4(\mu-CPh)_2]$ :  $d(WW) = 2.665(1) \text{ \AA}$ .
- [22] O. J. Scherer, M. Ehse, G. Wolmershäuser, *Angew. Chem.* **1998**, *110*, 530; *Angew. Chem. Int. Ed.* **1998**, *37*, 507.
- [23] G. Huttner, K. Everts, *Acc. Chem. Res.* **1986**, *19*, 406, and references therein, especially: H. Lang, L. Zsolnai, G. Huttner, *Angew. Chem.* **1983**, *95*, 1016; *Angew. Chem. Int. Ed. Engl.* **1983**, *22*, 976; G. Huttner, U. Weber, B. Sigwarth, O. Scheidsteger, H. Lang, L. Zsolnai, *J. Organomet. Chem.* **1985**, *282*, 331.
- [24] P. E. Garrou, *Chem. Rev.* **1985**, *85*, 171, and references therein.
- [25] P. E. Garrou, *Chem. Rev.* **1981**, 221.
- [26] E. D. Morrison, A. D. Harley, M. A. Marcelli, G. L. Geoffroy, A. L. Rheingold, W. C. Fultz, *Organometallics* **1984**, *3*, 1407.
- [27] A. M. Hinke, M. Hinke, W. Kuchen, *Z. Naturforsch. B.* **1986**, *41*, 629.
- [28] U. Nagel, *Chem. Ber.* **1982**, *115*, 1989.
- [29] P.-T. Cheng, S. C. Nyburg, *Can. J. Chem.* **1972**, *50*, 912.
- [30] For density functional calculations on the heteronuclear compounds we used the TURBOMOLE set of programs and applied the B-P86/SVP density functional within the RI-J approximation: a) R. Ahlrichs, M. von Arnim, „TURBOMOLE, Parallel Implementation of SCF, Density Functional, and Chemical Shift Modules“ in *Methods and Techniques in Computational Chemistry* (Eds.: E. Clementi, G. Corongiu) STEF, Cagliari, **1995**; b) K. Eichkorn, O. Treutler, H. Öhm, M. Häser, R. Ahlrichs, *Chem. Phys. Lett.* **1995**, *242*, 652. For definition of the B-P86 density functional see: c) A. D. Becke, *Phys. Rev. A* **1988**, *38*, 3098; d) J. P. Perdew, *Phys. Rev. B* **1986**, *33*, 8822; *erratum*: J. P. Perdew, *Phys. Rev. B* **1986**, *34*, 7406. The acronym SVP refers to TURBOMOLE split valence basis sets, augmented by a shell of polarization functions, compare: e) A. Schäfer, H. Horn, R. Ahlrichs, *J. Chem. Phys.* **1992**, *97*, 2571. Quasi-relativistic pseudo potentials were used for the elements W and Pt: see ref. [16].
- [31] H. Vahrenkamp, *Chem. Ber.* **1978**, *111*, 3472–3483.
- [32] a) S. Shaik, R. Hoffmann, *J. Am. Chem. Soc.* **1980**, *102*, 1194; b) S. Shaik, R. Hoffmann, C. R. Fisel, R. H. Summerville, *J. Am. Chem. Soc.* **1980**, *102*, 4555.
- [33]  $[(OC)_4W(\mu-PH_2)_2Pt(PH_3)]$  **11a** was also geometrically optimized by implementation of the RI-J-DFT method and with B-P86/SVP density functionals. Important calculated bond lengths and bond angles are:  $W-Pt$ : 2.851 Å,  $Pt-P$ : 2.39 Å,  $W-P$ : 2.553 Å,  $Pt-PH_3$ : 2.265 Å,  $P-Pt$ : 116.1°,  $P-W-P$ : 101.4°,  $W-P-Pt$ : 71.28°. Shared electron numbers were calculated: for two centers:  $W-Pt$ : 0.251,  $Pt-P$ : 0.452,  $Pt-PH_3$ : 0.472,  $W-P$ : 0.535; multi center contributions:  $Pt-W-P$ : 0.117,  $Pt-W-P-P$ : -0.044.
- [34] The shared electron number SEN is based on population analysis and can serve as a measure of covalent bond strength: R. Ahlrichs, C. Erhardt, *Chem. Unserer Zeit* **1985**, *19*, 120. Some typical values for SEN provided in this paper:  $C-C$ : 1.4;  $C-H$ : 2.2;  $C \equiv C$ ,  $N \equiv N$ : 3.3. Reduced SENs are found for polar bonds, like in  $NaF$  (0.3) and for weak bonds as in  $Cl_2$  (0.9) and  $F_2$  (0.6). For diborane  $H_2B(\mu-H)_2BH_2$  the SEN  $B-B$  provided is 1.66, which is mainly a result from three center contributions SEN  $B(\mu-H)B$  of 0.71. For the method employed here we calculate a SEN  $B-B$  of 1.58, and a SEN  $B(\mu-H)B$  of 0.68. Similar results as represented in the text for BP-RIDFT calculations can be obtained from BP-DFT, B3LYP-DFT, and HF calculations.
- [35] T. Allspach, M. Regitz, G. Becker, W. Becker, *Synthesis* **1986**, 31.
- [36] I. A. Latham, L. R. Sita, R. R. Schrock, *Organometallics* **1986**, *5*, 1508.
- [37] a) G. M. Sheldrick, *SHELXS-86*, University of Göttingen, **1986**; b) G. M. Sheldrick, *SHELXL-93*, University of Göttingen, **1993**.

Received: March 10, 1999, [F1665]